Journal of Statistical Physics. Vol. 68, Nos. 1/2, 1992

Quantum Qualitative Dynamics

Craig C. Martens[1]

Received October 3, 1991

We describe our work on qualitative methods for visualizing the quantum eigenstates of systems with nonlinear classical dynamics. For two-degree-of-freedom systems, our approach is based on the use of generalized coherent states, and allows systems with nonoscillator kinematics to be investigated. The general approach is illustrated with two examples involving vibration–rotation interaction in polyatomic molecules. We apply the coherent states of the Lie group $H_4 \otimes SU(2)$ to define quantum surfaces of section for a model involving centrifugal coupling of a harmonic bend with molecular rotation, and $SU(2) \otimes SU(2)$ coherent states to study two harmonic normal modes coupled to overall molecular rotation through coriolis interaction. In both systems, quantum states are visualized on the rotational surface of section and compared with the corresponding classical phase space structure. Striking classical–quantum correspondence is observed. We then describe recent results on the quantum states of $(N \geqslant 3)$-dimensional systems of coupled nonlinear oscillators, which reveal a quantum delocalization that is reminiscent of classical Arnold diffusion.

KEY WORDS: Classical–quantum correspondence; nonlinear dynamics; quantum chaos; phase space; coherent states; Arnold diffusion; Lie group theory.

1. INTRODUCTION

One of the most significant achievements of the physical sciences in the eighteenth century was the development of analytical mechanics.[1, 2] The work of Newton, Euler, Lagrange, Hamilton, and others made possible for the first time a consistent mathematical description of a broad range of

[1] Department of Chemistry, University of California-Irvine, Irvine, California 92717.

0022-4715/92/0700-0207$06.50/0

physical phenomena. The main inspiration for this advance came from celestial mechanics, and the prediction of heavenly events, such as eclipses and the periodic reappearances of comets, were dramatic examples of the success of analytical mechanics.

However, celestial mechanics also provided a profound defeat for analytical dynamics. This came about in attempts to investigate the long-time stability of the solar system. This n-body problem cannot be solved in closed form, and thus perturbative methods were used in an attempt to obtain an analytic description of planetary orbits that incorporated all significant gravitational interactions. During the last decades of the eighteenth century, it became clear that the perturbative approaches inevitably lead to divergent results. With the possibility of an analytical description of the n-body problem precluded, classical mechanics faced a crisis.

In an effort to circumvent this obstacle, the mathematician Henri Poincaré and a number of contemporaries developed a new approach to the study of dynamics.[3,4] The focus was changed from an effort to obtain analytic solutions for individual orbits using classical mathematical analysis to the study of the global geometric properties of vector fields in phase space and the topological structure of families of solutions to these equations of motion. The emphasis was on the organization of periodic orbits in phase space, their stability, and the bifurcations possible as system parameters were changed. A *qualitative* understanding of the geometry of dynamics was the goal of this new approach.[4]

Since its introduction, the qualitative theory of dynamical systems has been a powerful aid in proving theorems about the topology of orbits and invariant surfaces in phase space, their stability to small perturbations, and the possible modifications of this structure that bifurcations could induce.[4] More recently, with the increasing availability of computers, direct numerical solution to the equations of motion of nonlinear systems has become possible. This development greatly stimulated progress in dynamical systems theory, allowing a fruitful combination of numerical experiment and qualitative analysis. Many new phenomena have been discovered by "experimental mathematics" on the computer, providing direction for subsequent analysis and formal proof.[4]

For systems with two degrees of freedom, a particularly useful qualitative technique is the Poincaré surface of section,[4] which is a numerically-generated two-dimensional slice through the three-dimensional constant-energy subspace of the four-dimensional phase space. By computing families of trajectories having the same total energy but differing in their initial conditions, the foliation of phase-space organizing structures on the energy hypersurface can be visualized as they intersect the sectioning plane,

in much the same manner that a CAT scan allows the internal organization of the three-dimensional human body to be visualized.

The surface-of-section method has provided a great deal of insight into the dynamics of two-degree-of-freedom conservative systems. The details of the classical mechanics of many-dimensional systems (i.e., with three or more degrees of freedom) are less well understood.[5,6] Such systems cannot be visualized easily by the surface-of-section method, as the analogue of the two-dimensional section plane is a higher-dimensional hypersurface. Alternative ways of representing the results of computer experiments on many-dimensional dynamical systems are required.

The problems of interest in atomic, molecular, and nuclear physics are described by dynamical systems composed of particles interacting through nonlinear forces, and are thus similar in many ways to the problems of celestial mechanics. An essential difference, of course, is that these particles are submicroscopic, and thus require the use of quantum mechanics for a correct theoretical treatment. The mathematical structures of the conventional formulations of classical and quantum mechanics are vastly different: the canonical formalism of classical mechanics for an N-degree-of-freedom system is built around Hamilton's ordinary differential equations, whose solutions are trajectories in the $2N$-dimensional phase space of the system,[4] while quantum mechanics describes normalized eigenvectors in a (perhaps infinite-dimensional) Hilbert space,[7] which are often represented as a linear combination of a convenient set of basis states. In this form, quantum mechanics is not directly amenable to the qualitative analysis which is of such utility in classical mechanics.

In this paper, we describe our recent work on *quantum qualitative* methods. We discuss the general approach to two-degree-of-freedom systems, based on the use of generalized coherent states to define a quantum surface of section, and illustrate the method using two examples from the study of vibration–rotation eigenstates of polyatomic molecules.[8–10] We then present recent results from a continuing study of quantum–classical correspondence in high-dimensional systems, where the surface of section cannot be defined in a useful manner. We show a delocalization phenomenon of quantum states along resonance zones that is reminiscent of the classical Arnold diffusion mechanism of energy transport in ($N \geqslant 3$)-dimensional systems.[5,6]

Qualitative quantum mechanical methods have been applied in a number of studies investigating the correspondence principle in nonlinear systems. Inspection of wavefunctions in configuration space is a common technique, and effects such as the "scarring" of eigenstates by periodic orbits embedded in chaotic regions of phase space have been observed.[11] However, for a two-degree-of-freedom system, the two-dimensional

configuration space is a *projection* of the three-dimensional energy surface, and direct comparisons of quantum eigenstates and classical trajectories can be made difficult by quantum interference effects.[12]

Classical surfaces of section reveal the nature of phase space structure more clearly than configuration space trajectories, and phase space representation of quantum mechanics, evaluated on a *section* generated by the intersection of a two-dimensional plane with the three-dimensional energy shell, is often a more useful tool for analyzing the properties of quantum states. Such an approach can be based on the Wigner function,[13] a phase space representation of quantum mechanics. A related, and often more useful, quantity is the Husimi distribution.[14] The Husimi distribution is a locally averaged Wigner function, and has the advantages of being everywhere positive and more smoothly varying than the Wigner function.[14] In addition, the Husimi function is related to the coherent state representation of quantum mechanics.[15]

The Wigner and Husimi distributions have been employed previously in studies of classical–quantum correspondence in nonlinear dynamical systems. Hutchinson and Wyatt calculated a representation of the quantum states of the Hénon–Heiles potential that is related to the surface of section, but based on a projection instead of a section of phase space.[16] Weissman and Jortner constructed quantum surfaces of section of the Hénon–Heiles system using the coherent state representation of the harmonic oscillator.[17] Brown and Wyatt employed the Wigner function to represent the time evolution of a Morse oscillator driven by a periodic laser field.[18] Classical–quantum correspondence has been investigated in phase space for simple kicked systems, such as the standard map, by a number of authors.[19] Gray has compared classical phase space structure with the time evolution of the Wigner function for a periodically kicked one-dimensional Hamiltonian modeling vibrational predissociation of the van der Waals molecule HeI_2.[20] Lin an Ballentine employed the Husimi distribution to study coherent tunneling effects in a driven bistable system.[21] Benito *et al.* compared the classical and quantum phase space structure of the nonrigid molecule LiCN.[22] Stevens and Sundaram calculated a coarse-grained Wigner function to investigate the dynamics of driven surface-state electrons.[23] Skodje *et al.* used the coherent state representation to visualize quantum dynamics in their investigation of tunneling in a double-well problem.[24] The correlation between classical phase space structure and the phenomenology of "scarring" of quantum eigenstates by classical periodic orbits has been investigated for strongly chaotic systems by Waterland *et al.*,[25] who studied the two-dimensional quartic oscillator; Feingold *et al.*[26] and Davis *et al.*[27] considered the

idealized stadium and billiard systems from this perspective. Jensen has applied the Husimi representation to explore classical–quantum correspondence in atomic physics.[28] In related work, Kellman has developed methods to extract a classical-like phase space representation from fitting experimental spectra of polyatomic molecules.[29] Husimi and Wigner distributions for coupled oscillator systems have been described and reviewed by Davis *et al.*[27] and Davis.[30]

The work described here focuses on the extension of quantum surfaces of section to systems that are more general than coupled harmonic oscillators. To illustrate the method, we consider angular momentum-like degrees of freedom, whether physical rotation or a fictitious angular momentum derived from an $SU(2)$ representation of more general problems. We employ these generalized coherent states[15] to define *rotational* quantum surfaces of section, and use them to investigate vibration–rotation interaction mediated by centrifugal coupling in a rigid bender model.[8] In addition, we describe the representation of two nearly degenerate harmonic oscillators by an $SU(2)$ model, and investigate coriolis interaction of these vibrational degrees of freedom and overall molecular rotation by employing $SU(2) \otimes SU(2)$ coherent states.[9,10] Generalizations of phase space representations of quantum mechanics to nonoscillator kinematics have also been considered by Kurchan *et al.*[31]

The organization of this paper is as follows: in Section 2 we briefly describe a definition of generalized coherent states based on the theory of Lie groups. In Section 3 we review the definition of a classical surface of section for a two-degree-of-freedom system and describe the construction of an analogous quantum surface of section using generalized coherent states. Section 4 illustrates this general approach using coherent states of the direct product group $H_4 \otimes SU(2)$, appropriate for a harmonic oscillator coupled to a rotational degree of freedom, to construct quantum surfaces of section for a rigid bender model of an ABA triatomic molecule undergoing centrifugal vibration–rotation coupling. These are compared with a classical surface of section calculated for the same model. Section 5 then describes a coupled spin model for coriolis-induced vibration–rotation interaction, based on an $SU(2)$ representation of the two-dimensional harmonic oscillator. The coherent states of $SU(2) \otimes SU(2)$ are then employed to the study the quantum states of this system. In Section 6 we consider the relatively unexplored problem of classical–quantum correspondence in many-dimensional systems by investigating a model Hamiltonian describing three coupled nonlinear oscillators. Surfaces of section are not readily applicable in this case. An alternative method for investigating classical–quantum correspondence is described, and applied

to reveal quantum delocalization that is suggestive of the classical mechanism of transport in ($N \geqslant 3$)-dimensional systems known as Arnold diffusion. Finally, a discussion is given in Section 7.

2. GENERALIZED COHERENT STATES

The connection between classical and quantum mechanics can be made by considering quantum states which, in some sense, are as "classical" as possible—states that are as localized in phase as permitted by the uncertainty principle $\Delta q\, \Delta p \geqslant \hbar/2$.[7] The *coherent states* constitute such a representation.[15] The most familiar coherent states are those of the one-dimensional harmonic oscillator, which are minimum-uncertainty wave packets localized in both position and momentum. This maximal localization in phase space allows the center of these states, in the limit $\hbar \to 0$, to be interpreted as classical variables.

The coherent states of the harmonic oscillator are defined as minimum-uncertainty states, or alternatively, as eigenstates of the annihilation operator.[15] An equivalent definition[15] expresses the coherent states as a displaced oscillator ground state, generated by the action of a unitary operator $U(z)$:

$$|z\rangle = U(z)\,|0\rangle \tag{1}$$

with $U(z)$ given by

$$U(z) = \exp(za^\dagger - z^* a) \tag{2}$$

Here, $a^\dagger$ and a are the harmonic oscillator creation and annihilation operators and $z = (q + ip)/\sqrt{2}$ is a complex number. The operator $U(z)$ displaces the state $|0\rangle$ without changing its shape or minimum-uncertainty character. The two real parameters (q, p) are interpreted as the center of the state in a classical phase space. The states $|z\rangle$ can be expanded in a basis of eigenstates of the number operator $a^\dagger a$:

$$|z\rangle = e^{-|z|^2/2} \sum_{n=0}^{\infty} \frac{z^n}{(n!)^{1/2}}\,|n\rangle \tag{3}$$

The definition of the harmonic oscillator coherent states is represented schematically in Fig. 1.

The harmonic oscillator coherent states can be generalized to other systems in a number of ways. Some approaches are based on the requirement of minimum uncertainty, while other definitions require the generalized coherent states to be eigenvectors of a lowering or annihilation

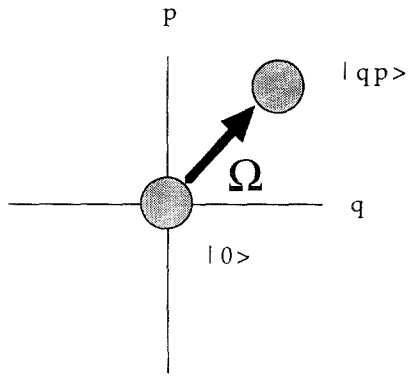

Fig. 1. A schematic view of the definition of harmonic oscillator coherent states. The states are generated by the action of the unitary operator Ω on the minimum-uncertainty harmonic oscillator ground state. The transformation displaces the state to a position $z = (q, p)$ on the complex plane, while retaining its shape and minimum-uncertainty character. The point (q, p) is the interpreted as a set of canonical variables in classical phase space.

operator.[15] For our purposes, the most convenient approach is based on defining generalized coherent states as displaced extreme states in a Hilbert space which carries an irreducible representation of a particular Lie group.[15,32] We now summarize this group-theoretic definition of generalized coherent states.

Let g be an element of the Lie group $\mathcal{G}$. In practice, g will be given as an exponential of an anti-Hermitian linear combination of the generators of the group $\mathcal{G}$ (i.e., a set of operators closed under commutation). Let $|\Phi_0\rangle$ be a reference state in the Hilbert space of the physical problem. The stability subgroup $\mathcal{H}$ of $\mathcal{G}$ with respect to the state $|\Phi_0\rangle$ is then defined as the set of all group elements of $\mathcal{G}$ which leave $|\Phi_0\rangle$ invariant, up to a phase:

$$h|\Phi_0\rangle = |\Phi_0\rangle e^{i\phi(h)} \qquad (h \in \mathcal{H}) \tag{4}$$

The coset space of $\mathcal{G}$ is then the quotient $\mathcal{G}/\mathcal{H}$, so that every group element g can be written as the product of an element in $\mathcal{H}$ and an element of $\mathcal{G}/\mathcal{H}$:

$$g = \Omega h \qquad (g \in \mathcal{G}, \quad h \in \mathcal{H}, \quad \Omega \in \mathcal{G}/\mathcal{H}) \tag{5}$$

The coherent states $|\omega\rangle$ of $\mathcal{G}$ are then defined as the states generated by operating on $|\Phi_0\rangle$ with an operator $\Omega \in \mathcal{G}/\mathcal{H}$:

$$|\omega\rangle = \Omega|\Phi_0\rangle \tag{6}$$

where ω denotes a set of group parameters labeling the state. The operator Ω is an exponential of an anti-Hermitian linear combination of a subset of the generators of the group $\mathcal{G}$, and the group parameters are related to the coefficients of these generators. In the work described here, the parameters ω shall always be chosen to be canonical coordinates, and thus directly comparable to the phase space variables of the corresponding classical system.

The coherent states of the harmonic oscillator are a special case of this general definition.[15] Here, the group $\mathcal{G}$ is H_4, the Heisenberg–Weyl group. The generators of H_4 are a and $a^\dagger$, the annihilation and creation operators, the number operator $n = a^\dagger a$, and the identity operator $\mathbb{1}$. The reference state is the oscillator ground state $|0\rangle$. The number and identity operators generate the stability subgroup, and the operators Ω are given by Eq. (2). The group parameters are the coordinates q and p, the real and imaginary parts of z.

We now describe the generalization of the oscillator coherent state to problems involving rotational dynamics. The appropriate Lie group for rotations is $SU(2)$, which is homomorphic to the rotation group $SO(3)$. The generators of $SU(2)$ are the angular momentum components J_x, J_y, and J_z. A reference state in the $(2j+1)$-dimensional Hilbert space spanned by the states $\{|jm\rangle\}$ $(m = -j,..., j)$, which are eigenstates of $J^2 = J_x^2 + J_y^2 + J_z^2$ and J_z, is the minimum-uncertainty state $|j-j\rangle$. The operator J_z generates the stability subgroup. The coherent states of $SU(2)$ are given by the action of a unitary operator on the reference state $|j-j\rangle$:

$$|\theta\phi\rangle = U(\theta, \phi)\,|j-j\rangle \tag{7}$$

where

$$\begin{aligned} U(\theta, \phi) &= \exp(\zeta J_+ - \zeta^* J_-) \\ J_\pm &= J_x \pm i J_y \\ \zeta &= \frac{\theta}{2} e^{-i\phi} \end{aligned} \tag{8}$$

Here, θ and ϕ are the polar and azimuthal angles on the unit sphere. The states $|\theta\phi\rangle$ can be expanded in the basis of eigenstates of J^2 and J_z:

$$|\theta\phi\rangle = \sum_{m=-j}^{j} \binom{2j}{j+m}^{1/2} \sin^{j+m}(\theta/2) \cos^{j-m}(\theta/2) e^{-i(j+m)\phi}\,|jm\rangle \tag{9}$$

In order to compare with classical Hamiltonian mechanics, the geometrical angles θ and ϕ must be transformed to canonical variables

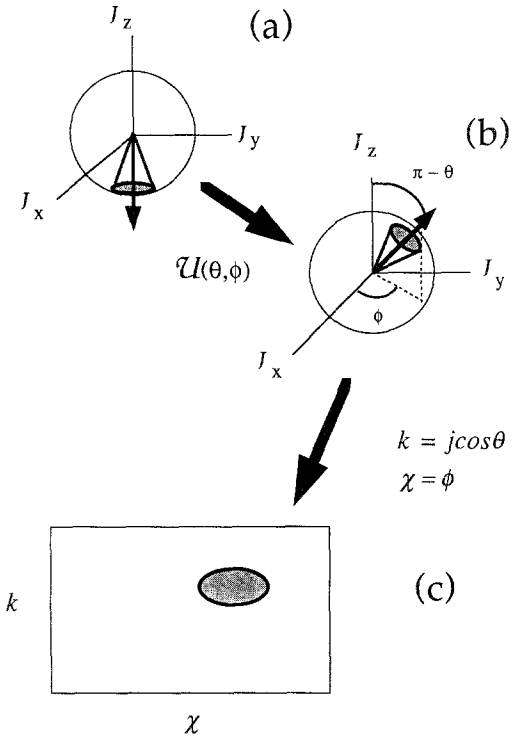

Fig. 2. A schematic view of the definition of $SU(2)$ coherent states. (a) The states are generated by the action of the unitary operator $U(\theta, \phi)$ on the state $|j-j\rangle$, an eigenstate of J_z with minimum uncertainty in the x and y components of **J**. (b) The transformation rotates the state to an arbitrary position on the angular momentum sphere, while retaining its shape and minimum uncertainty. (c) The surface of each sphere is related to a phase plane through a transformation to canonical coordinates.

(k, χ) obeying the proper Poisson bracket relations.[33] The transformation is given by $\chi = \phi$ and $k = -j \cos\theta$.[8,9] Physically, k is the projection of the angular momentum on the z axis, and χ is the canonically conjugate angle.

Figure 2 shows schematically the definition of $SU(2)$ coherent states.

3. QUANTUM SURFACES OF SECTION

A classical surface of section for a two-degree-of-freedom Hamiltonian system is constructed by integrating Hamilton's equations of motion for a family of trajectories with the same initial energy but differing initial conditions. Each trajectory is followed through phase space, and the intersections of the orbit with a plane in phase space (the surface-of-section plane)

are determined. A composite plot of these points for the family of trajectories gives a numerical representation of the underlying invariant surfaces resulting from additional constants of the motion beyond energy conservation, or, if the system is chaotic, an indication of the absence of additional constants of the motion. The classical surface of section gives a clear indication of the existence of important phase structures, such as nonlinear resonance zones, stable or unstable periodic orbits, and regions of chaotic motion.

Generalized coherent states can be employed to define a quantum analogue of the classical surface of section. Here, the invariant quantum density of an eigenstate is visualized and compared with the invariant tori, stable and unstable manifolds, and other time-independent structure on the classical surface of section. By interpreting the center of the coherent state as classical canonical coordinates (q, p), the structure of quantum Hilbert space can be revealed in a manner that is directly analogous to the classical surface of section. This is accomplished by projecting the state $|\psi\rangle$ of interest onto the coherent state probe:

$$\rho(q, p) = |\langle qp|\psi\rangle|^2 \tag{10}$$

The parameters q and p are then interpreted as being classical phase space variables. The key point is that the state $|\psi\rangle$ has been mapped onto a classical-like representation: probability density as a function of the canonical variables q and p.

For two-degree-of-freedom systems, a quantum surface of section can be defined which allows a parallel comparison of the classical phase space structure and quantum eigenstate morphology. In this case, the probe states are just the direct product of two one-degree-of-freedom coherent states: $|q_1 q_2 p_1 p_2\rangle = |q_1 p_1\rangle \,|\, q_2 p_2\rangle$, and are thus parametrized by four real numbers. These numbers are interpreted as the generalized coordinates and conjugate generalized momenta of the corresponding four-dimensional classical phase space. A probability density is then defined as

$$\rho(q_1, q_2, p_1, p_2) = |\langle q_1 q_2 p_1 p_2|\psi\rangle|^2 \tag{11}$$

If $|\psi\rangle$ is an eigenstate of a system with energy eigenvalue E, then quantum surface of section can be computed by "slicing" this multidimensional function in a manner directly analogous to the way a classical surface of section is calculated. This is accomplished by constraining the coherent state parameters (q_1, q_2, p_1, p_2) to lie on the analogue of the classical surface of section, using the following conditions:

(i) $q_2 = 0$ and $p_2 > 0$ (surface-of-section plane).

(ii) $H(q_1, q_2, p_1, p_2) = E$ (energy hypersurface).

Here H is the expectation value of the Hamiltonian in the coherent state basis and E is the quantum energy eigenvalue. The resulting *surface-of-section* probability density $\rho(q_1, p_1)$ is a function of two variables, and can be visualized by computing a contour plot.

4. CENTRIFUGAL COUPLING IN ABA MOLECULES

In this section, we illustrate the general approach by calculating quantum surfaces of section for a simple model of centrifugal coupling of the bend vibration of an ABA triatomic molecule with overall rotation.[8] In this idealized system, a harmonic bend degree of freedom interacts with the rotation of the molecule through the dependence of the molecular moments of inertia on the bend angle. The Hamiltonian considered is given by[8]

$$H = \tfrac{1}{2}(p^2 + \omega^2 q^2) + A(q)J_z^2 + B(q)J_y^2 + C(q)J_x^2 \tag{12}$$

where A, B, and C are the molecular rotational constants, $q = \theta - \theta_0$ is the deviation of the bend angle of the molecule from its equilibrium value, p is the conjugate bend momentum, and (J_x, J_y, J_z) are the components of the total angular momentum of the system, expressed in the body-fixed principal axis frame.[34] The dependence of the rotational constants on q is given by Taylor series expansion though quadratic terms. More details and numerical values for the parameters in the Hamiltonian are given in ref. 8.

The components of the classical total angular momentum J are not a suitable set of canonical momenta, as they do not have mutually vanishing Poisson brackets,[33] obeying instead

$$\begin{aligned} \{J_x, J_y\} &= -J_z \\ \{J_y, J_z\} &= -J_x \\ \{J_z, J_x\} &= -J_y \end{aligned} \tag{13}$$

where the minus sign results from the body-fixed coordinate system.[8,9,34] A suitable set of canonical coordinates for rotation are (χ, k), which are related to the components of the angular momenta by the transformation

$$\begin{aligned} J_x &= (J^2 - k^2)^{1/2} \cos(\chi) \\ J_y &= -(J^2 - k^2)^{1/2} \sin(\chi) \\ J_z &= k \end{aligned} \tag{14}$$

Physically, k is the projection of the total angular momentum vector on the body-fixed z axis, and χ is the conjugate angle variable.

Figure 3a shows a classical surface of section for this system, calculated by integrating a family of trajectories at a fixed energy and plotting (χ, k) for each trajectory when $q=0$ and $p>0$. The surface of section shows rich phase space structure, including prominent resonance zones for $k \cong 30$ and layer of chaotic dynamics surrounding the two large

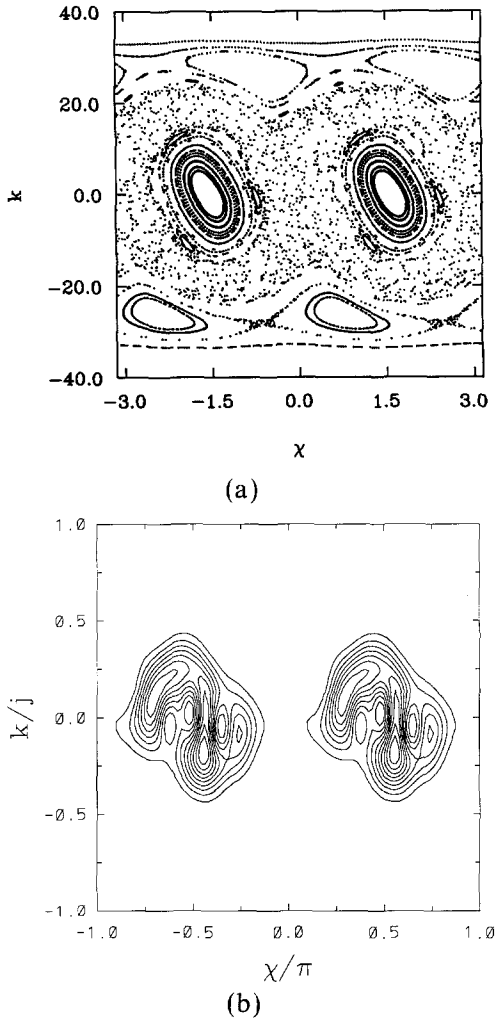

Fig. 3. (a) Classical surface of section for two-mode ABA triatomic molecule. (b) Quantum surface of section showing a state localized on the large elliptic region around $k=0$. (c) Quantum surface of section showing a state localized on island of the 2:1 resonance zone. (d) Quantum surface of section showing a state localized on 2:1 unstable periodic orbits and emanating stable and unstable manifolds.

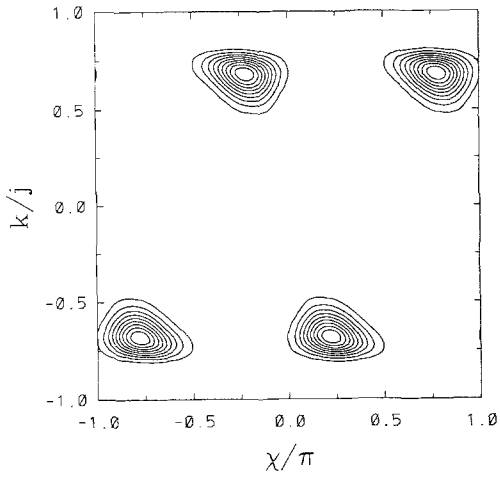

(c)

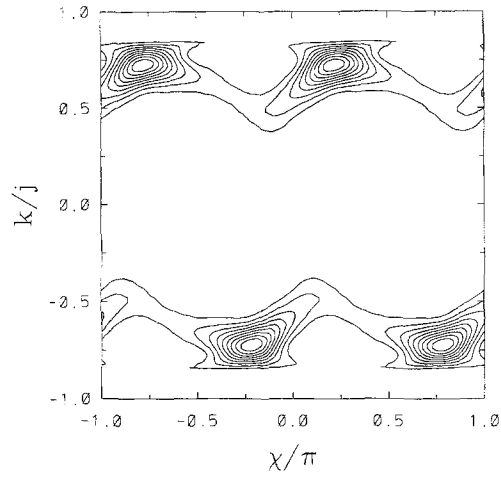

(d)

Fig. 3 (*continued*)

stable elliptic regions of phase centered at $k=0$, corresponding physically to rotation of the molecule around the body-fixed x axis.

This system consists of a harmonic vibration coupled to molecular rotation. Quantum surfaces of section for this system can thus be calculated by employing the generalized coherent states $|qp\chi k\rangle = |qp\rangle\,|\chi k\rangle$ of the direct product Lie group $H_4 \otimes SU(2)$. A rotational surface-of-section probability density $\rho(\chi, k)$ for the state ψ_α is calculated by evaluating

the projection $\rho(q, p, \chi, k) = |\langle qp\chi k | \psi_\alpha \rangle|^2$, subject to the additional conditions $q = 0$, $p > 0$ (surface-of-section plane condition), and $\langle qp\chi k | H | qp\chi k \rangle = E_\alpha$, where E_α is the quantum energy eigenvalue of the state ψ_α, and is set equal to the expectation value of the Hamiltonian in the coherent state basis (energy surface condition).

In Figs. 3b–3d we show contour plots of the surface-of-section probability densities calculated for three quantum eigenstates of Eq. (12) with energies very close to the classical energy used in Fig. 3a. Each state is localized in a different region of phase space. The structure of the states closely parallels the corresponding classical behavior. Figure 3b shows a state localized on the large elliptic regions around $k = 0$. Figure 3c gives an eigenstate which is centered on the chain of islands resulting from a 2:1 resonance between vibration and rotation. The state shown in Fig. 3d is localized on the unstable periodic orbits and emanating manifolds making up the broken separatrix around the 2:1 resonances zones.

These figures show a strong correspondence between the detailed structure of classical phase space, as seen through the Poincaré surface of section, and the localization of the corresponding quantum states, as visualized by quantum qualitative analysis. Most of the remaining eigenstates of the system show a similar correlation with underlying classical behavior.

5. COUPLED SPIN MODEL OF CORIOLIS INTERACTION

In this section, we provide another illustration of classical–quantum correspondence in molecular vibration–rotation dynamics. Here, we consider the coriolis coupling of two nearly degenerate harmonic vibrations by interaction with overall molecular rotation. A simplified Hamiltonian that captures the general physical features of this problem is given by[9,10]

$$H = \frac{\omega_1}{2}(p_1^2 + q_1^2) + \frac{\omega_2}{2}(p_2^2 + q_2^2) + A_0 J_z^2 + B_0 J_y^2 + C_0 J_x^2 - 2A_0 \pi_z J_z \quad (15)$$

where (q_1, q_2) are two normal coordinates of the molecule, (p_1, p_2) are the conjugate momenta, ω_1 and ω_2 are the normal mode frequencies, (J_x, J_y, J_z) are the components of the total angular momentum, and A_0, B_0, and C_0 are the molecular rotational constants. Coriolis coupling results from the interaction of the total angular momentum $\mathbf{J}$ and the vibrational angular momentum $\boldsymbol{\pi}$.[34] The only term allowed by the symmetry of the model considered[9,10] is the product of the z components of the two angular momenta, and appears as the last term of Eq. (15). The z

component of the vibrational angular momentum depends on the normal coordinates and momenta, and is given approximately by

$$\pi_z = \zeta(q_1 p_2 - q_1 p_1) \tag{16}$$

where ζ is the coriolis coupling parameter. Although the system depends on three degrees of freedom, conservation of the total vibrational action reduces the problem to two dimensions, and so the surface-of-section technique can be applied.

To make this dimensional reduction apparent, we transform to the system to a "coupled spin" Hamiltonian[8,10] by using the $SU(2)$ representation of two-dimensional harmonic oscillators.[32,35] We define the three components of a second angular momentum through the transformation equations

$$\begin{aligned} S_x &= \tfrac{1}{2}(q_1 p_2 - q_2 p_1) \\ S_y &= \tfrac{1}{2}(q_1 q_2 + p_1 p_2) \\ S_z &= \tfrac{1}{4}(p_2^2 + q_2^2 - p_1^2 - q_1^2) \end{aligned} \tag{17}$$

The conservation of the total vibrational action is equivalent to the constancy of the length of the angular momentum $S^2 = S_x^2 + S_y^2 + S_z^2 = s(s+1)$. Using this transformation, the Hamiltonian becomes

$$2\omega(s + \tfrac{1}{2}) + 2\delta S_z + A_0 J_z^2 + B_0 J_y^2 + C_0 J_x^2 - 4A_0 \zeta S_x J_z \tag{18}$$

A set of canonical coordinates for this coupled angular momentum problem is given by a two-dimensional generalization of Eq. (14),[9,10]

$$\begin{aligned} S_x &= (S^2 - k_1^2)^{1/2} \cos(\chi_1) \\ S_y &= (S^2 - k_1^2)^{1/2} \sin(\chi_1) \\ S_z &= k_1 \end{aligned} \tag{19}$$

$$\begin{aligned} J_x &= (J^2 - k_2^2)^{1/2} \cos(\chi_2) \\ J_y &= -(J^2 - k_2^2)^{1/2} \sin(\chi_2) \\ J_z &= k_2 \end{aligned} \tag{20}$$

In Fig. 4a we show a classical surface of section calculated for this system with the classical angular momenta having values $s = 10$, $j = 40$. (See ref. 9 for further details.) This surface of section corresponds to the molecular rotational degree of freedom. A mixture of nonresonant, resonant, and chaotic dynamics is seen, resulting from strong breakdown

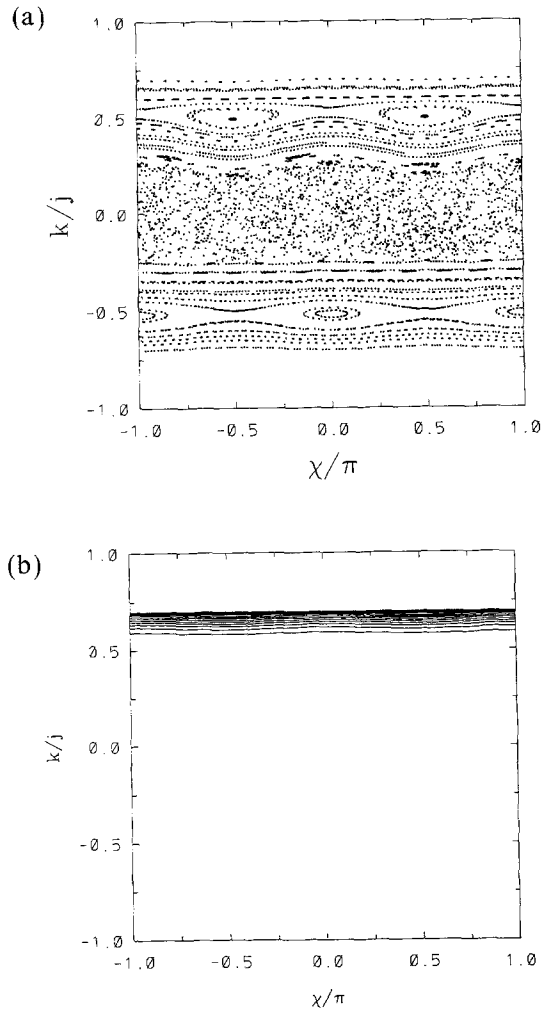

Fig. 4. (a) Classical surface of section for coupled spin model of coriolis interaction in polyatomic molecule. (b) Quantum surface of section showing a state localized on non-resonant tori at extreme allowed value of k_2. (c) Quantum surface of section showing a state localized on islands resulting from resonant interaction between vibration and rotation. (d) Quantum surface of section showing a state localized on unstable periodic orbits and emanating stable and unstable manifolds. (e) Quantum state located in the region of classical chaos.

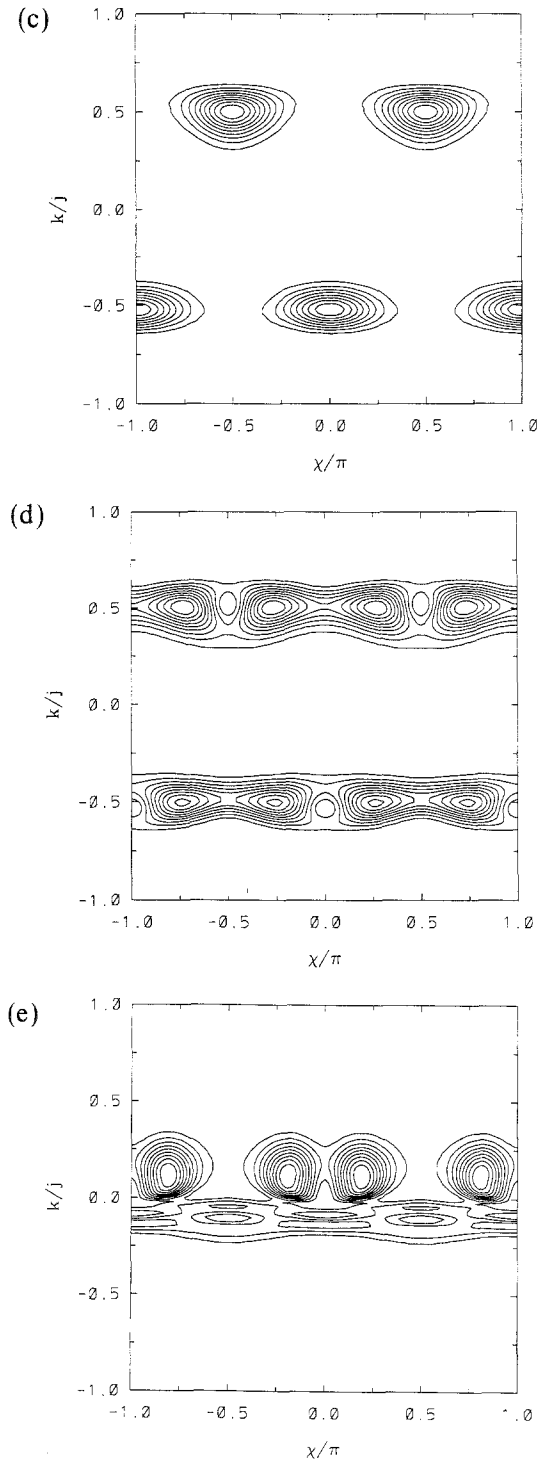

Fig. 5. (*Continued*)

of the separation of vibrational and rotational motion in this system. In particular, prominent 2:1 resonance zones are observed for $|k_2/j|$ approximately equal to 0.5, while near $k=0$ a broad region of chaos is visible.

This system consists of two coupled angular momentum degrees of freedom. To calculate quantum surfaces of section for this system, the generalized coherent states of the direct product group $SU(2)\otimes SU(2)$ are used, defined as the product of two 1-dimensional $SU(2)$ coherent states: $|\chi_1\chi_2 k_1 k_2\rangle = |\chi_1 k_1\rangle\,|\chi_2 k_2\rangle$.[10] The surface-of-section and energy constraints are applied in the same manner as in the previous example.

Figures 4b–4e give the (χ_2, k_2) quantum surfaces of section for four eigenstates of this system with eigenvalues near the classical energy used to compute Fig. 4a. Figure 4b shows a state that is localized on a nonresonant invariant torus near the extreme value of k_2 allowed at the energy considered. In Fig. 4c another state is given. Here, the probability density is large in the 2:1 resonant region of phase, and is centered on the stable elliptic islands. The state shown in Fig. 4d is also localized in the 2:1 resonant region of the surface of section, but is associated with the unstable 2:1 periodic orbits and their stable and unstable manifolds. Figure 4e shows a state that is situated in the chaotic portion of phase space. The state shows additional structure and localization, perhaps due to the effect of unstable periodic orbits embedded in the chaotic region.[11,25,26]

The second example provides another illustration of the pronounced effect that classical nonlinear dynamics can have on the structure of polyatomic molecular vibration–rotation eigenstates. These effects are convincingly revealed in these two-degree-of-freedom systems by the application of quantum qualitative analysis, as a direct comparison of the classical surface of section with its quantum analogue can be made. In the next section, we address the extension of qualitative methods to the investigation of systems with more than two degrees of freedom, where the surface-of-section approach described here cannot be applied.

6. CLASSICAL–QUANTUM CORRESPONDENCE IN MANY-DIMENSIONAL SYSTEMS

The nonlinear dynamics of two-degree-of-freedom systems is at present fairly well understood.[4,36] The current level of understanding is due, to a great extent, to the successful application of numerical simulation combined with methods of qualitative dynamics—in particular, the surface-of-section approach. Although great advances have been made in nonlinear dynamics by the study of two-degree-of-freedom problems and related

area-preserving surface-of-section mappings, much of this detailed understanding is of relevance only to the special case $N=2$.

The important differences between two-mode systems and systems with three or more degrees of freedom are due to the dimensionality of the phase space structures governing dynamical behavior. For an N-degree-of-freedom system, the phase space is $2N$-dimensional. The energy hypersurface is defined by the single constraint equation $H(q, p)=E$, and thus is a $(2N-1)$-dimensional subspace of the full phase space. Invariant tori are characterized by a complete set of N constants of the motion, and thus restrict the dynamics to $(2N-N=N)$-dimensional subspaces. For $N=2$, N-dimensional tori divide the $(2N-1)$-dimensional energy shall into disjoint regions; no chaotic trajectory can cross an intact 2-torus to reach the region of the three-dimensional energy shell on the other side, and "leaky" tori, called cantori,[36] can act as bottlenecks to energy transport. This occurs because, for two degrees of freedom, $2N-2$ (the dimension of a dividing surface on the energy shell) is equal to N (the dimension of an invariant torus).

For $N \geqslant 3$, however, tori (or cantori) do not have the proper dimensionality to act as dividing surfaces on the energy shell. A chaotic trajectory can avoid an intact torus simply by going around it. Any dividing surface in higher-dimensional systems must be made of continuous families of such N-dimensional invariant surfaces. As shown by Kolmogorov, Arnold, and Moser,[4,36] a finite measure of the invariant tori filling the phase space of an integrable nonlinear system survives when a nonintegrable perturbation is added. The survivors are located in regions where the ratios of the frequencies of motion are sufficiently irrational. Tori with frequencies in resonance are destroyed by the perturbation. Although the KAM theorem guarantees that, for sufficiently small perturbations, some tori will persist, number theory tells us that rational numbers are densely distributed among real numbers, and thus there are destroyed tori between any two persistent ones. Therefore, strict dividing surfaces cannot exist in $(N \geqslant 3)$-degree-of-freedom systems; they are everywhere pierced by destroyed rational tori. The network of destroyed rational tori is called the Arnold web, and makes possible energy transport throughout the entire phase space. This process is called Arnold diffusion.[4,5,36]

Another factor complicating the study of many-dimensional systems is that the surface-of-section technique cannot be applied to visualize phase space structure on a two-dimensional plot, as a slice through a higher-dimensional energy hypersurface will itself have a dimension greater than two. This problem of visualization, coupled with the new phenomena present, has left many unanswered questions and outstanding problems in the theory of many-dimensional Hamiltonian dynamics.[4–6]

To make progress in the classical and quantum qualitative analysis of many-dimensional systems, alternative methods of visualization must be employed. These must, of necessity, reduce the number of phase space variables considered. In this section, we describe an approach to $(N=3)$-dimensional systems that allows comparison of classical phase space structure and quantum mechanical eigenstates.

We consider a system consisting of three coupled nonlinear oscillators modeling highly excited molecular vibrations. The classical Hamiltonian is of the form

$$H(\mathbf{I}, \theta) = H_0(\mathbf{I}) + H'(\mathbf{I}, \theta) \tag{21}$$

where $\mathbf{I} = (I_1, I_2, I_3)$ and $\boldsymbol{\theta} = (\theta_1, \theta_2, \theta_3)$ are the action and angle variables of the zeroth-order Hamiltonian H_0. In terms of the action–angle variables, the classical Hamiltonian is given by

$$H_0(\mathbf{I}) = \Omega_1 I_1 + \Omega_2 I_2 + \Omega_3 I_3 + \tfrac{1}{2}\alpha_1 I_1^2 + \tfrac{1}{2}\alpha_2 I_2^2 + \alpha_3 I_3^2 \tag{22}$$

$$H'(\mathbf{I}, \boldsymbol{\theta}) = 2\beta_1 (I_1^2 I_2)^{1/2} \cos(2\theta_1 - \theta_2) + 2\beta_2 (I_1^3 I_2^2)^{1/2} \cos(3\theta_1 - 2\theta_2) + 2\beta_3 (I_2 I_3^2)^{1/2} \cos(\theta_2 - 2\theta_3) \tag{23}$$

where the β_i are coupling parameters. The zeroth-order Hamiltonian H_0 corresponds to a set of three uncoupled anharmonic oscillators with harmonic frequencies $(\Omega_1, \Omega_2, \Omega_3)$ and anharmonicities $(\alpha_1, \alpha_2, \alpha_3)$. The actual frequencies of the oscillators depend on action, and are given by

$$\omega_j(\mathbf{I}) = \frac{\partial H_0(\mathbf{I})}{\partial I_j} \qquad (j = 1, 2, 3) \tag{24}$$

The perturbation $H'(\mathbf{I}, \boldsymbol{\theta})$ consists of three resonant terms, which are of the general form $f_k(\mathbf{I}) \cos(\mathbf{k} \cdot \boldsymbol{\theta})$, where $f_k(\mathbf{I})$ is a function of action and $\mathbf{k}$ is a vector with integer components. Each resonant term will have a significant effect in regions of phase space where the frequencies $\omega(\mathbf{I})$ satisfy the resonance condition $\mathbf{k} \cdot \boldsymbol{\omega} = 0$. Here, the phase of the resonant term is slowly varying, allowing the resonance to have a large effect on the dynamics. A system with a single resonance term can be transformed to a one-dimensional action–angle problem, and is thus integrable. The addition of further resonance terms destroys the integrability, however, and all global constants of the motion beyond the Hamiltonian itself will be destroyed in the presence of three independent resonance terms.

The phase space of this classical system has six dimensions, and is therefore not easily visualized. Physically, the most important characteristics of the dynamics are the rate and extent of energy exchange

between the modes. Thus, the mode energies, or equivalently, the zeroth-order oscillator actions, are of greatest interest; the angle variables describing the accompanying phases are of less importance. We shall therefore suppress the angle variables and view a reduced action space of the full phase space in our qualitative analysis of this system.

Figure 5 shows a schematic view of the action space of the system. For a small perturbation, the zeroth-order energy H_0 is approximately conserved. This condition constrains the dynamics in action space to lie on or near the zeroth-order energy shell $H_0 = E$. This is a two-dimensional surface in the three-dimensional action space, as indicated. Resonance conditions $\mathbf{k} \cdot \boldsymbol{\omega} = 0$ give, for each $\mathbf{k}$, an independent condition among the three actions. The results is a set of 2-dimensional resonance surfaces in action space. The intersections of these surfaces with the zeroth-order energy surface result in a set of resonance lines on the energy shell. Three such resonance lines have been indicated in the figure. The presence of a single resonance term in H causes a resonance zone to form. A resonance zone can be approximately described as the librational portion of a pendulum phase portrait; the zeroth-order actions experience extensive periodic oscillations inside of the resonance zone in the single resonance case. The maximum extent of these oscillations is given by the resonance width. The widths of the resonance zones are also indicated schematically in Fig. 5.

The union of the resonance zones for all $\mathbf{k}$ constitutes the Arnold web.[4,6] Numerical studies on three-dimensional nonlinear systems indicate that energy transport occurs predominantly *along* these resonance lines.[4,6]

We now describe the calculation and visualization of eigenstates for

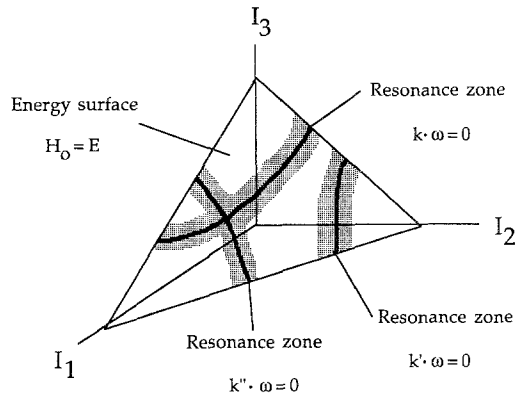

Fig. 5. A schematic view of phase space structure, as seen in a reduced action space, for a three-degree-of-freedom nonlinear coupled oscillator problem. See the text for discussion.

the quantum version of this system. The quantum Hamiltonian operator can be written in terms of creation and annihilation operators as

$$H_0(\mathbf{I}) = \Omega_1(a_1^\dagger a_1 + \tfrac{1}{2}) + \Omega_2(a_2^\dagger a_2 + \tfrac{1}{2}) + \Omega_3(a_3^\dagger a_3 + \tfrac{1}{2}) + \tfrac{1}{2}\alpha_1(a_1^\dagger a_1 + \tfrac{1}{2})^2 + \tfrac{1}{2}\alpha_2(a_2^\dagger a_2 + \tfrac{1}{2})^2 + \alpha_3(a_3^\dagger a_3 + \tfrac{1}{2})^2 \quad (25)$$

$$H'(\mathbf{I}, \theta) = \beta_1[(a_1^\dagger)^2 a_2 + a_1^2 a_2^\dagger] + \beta_2[(a_1^\dagger)^3 a_2^2 + a_1^3(a_2^\dagger)^2] + \beta_3[a_2^\dagger a_3^2 + a_2(a_3^\dagger)^2] \quad (26)$$

The equivalence of Eqs. (25) and (26) and the classical Hamiltonian functions (22) and (23) can be seen by making the following identification between action–angle variables and the classical analogue of the creation and annihilation operators:

$$a_j = I_j^{1/2} e^{-i\theta_j}$$
$$a_j^\dagger = I_j^{1/2} e^{i\theta_j} = a_j^* \qquad (j = 1, 2, 3) \quad (27)$$

where a_j^* is the complex conjugate of a_j.

The time-independent Schrödinger equation was solved by diagonalization of H in a basis of eigenstates $\{|n_1 n_2 n_3\rangle\}$ of the zeroth-order part H_0. A nonvariational basis, consisting of a band of zeroth-order states centered around the energy range of interest, was used. Convergence of the calculations was checked by increasing the basis size.

Due to the high dimensionality of phase space, the quantum surface-of-section method cannot be applied to visualize the eigenstates of H, and an alternative must be found. We stated above that the most important aspects of the classical dynamics can be represented in the space of zeroth-order action variables, and that the phases of the oscillators are of less importance. We use the analogous approach here, and visualize the states in zeroth-order *quantum number* space, which is related to action space through the semiclassical quantization relations $I_j = (n_j + 1/2)\hbar$.

For weak perturbations, classical action trajectories remain on or near the surface $H_0 = E$. Thus, the features viewed in the full three-dimensional action space can be represented approximately on a two-dimensional surface. This can be accomplished by projecting the full action space onto the (I_1, I_2) plane. In a similar manner, we visualize the eigenstates of H on the (n_1, n_2) quantum number plane. For a state $|\psi\rangle$, we define a probability density depending on the three zeroth-order quantum numbers $\rho(n_1, n_2, n_3)$ as

$$\rho(n_1, n_2, n_3) = |\langle n_1 n_2 n_3 | \psi \rangle|^2 \quad (28)$$

This quantity is equal to $|c(n_1, n_2, n_3)|^2$, the square of the appropriate coefficient of the basis state $|n_1 n_2 n_3\rangle$ in the expansion of eigenstate $|\psi\rangle$:

$$|\psi\rangle = \sum_{n_1 n_2 n_3} c(n_1, n_2, n_3)|n_1 n_2 n_3\rangle \tag{29}$$

This representation loses information about the *phase* of the contribution of the basis state to the eigenstate, just as the classical action space contains no information on the relative phases of the oscillators. To project the probability density onto the (n_1, n_2) plane, we sum over the third zeroth-order quantum number n_3:

$$\rho(n_1, n_2) = \sum_{n_3} \rho(n_1, n_2, n_3) \tag{30}$$

A contour plot of this probability density can then be made, and compared with the expected classical phase space structure.

In Figs. 6 and 7, we show eigenstates for cases where only a single resonance term is included in the Hamiltonian. Using the semiclassical quantization condition $I_j = (n_j + 1/2)\hbar$, we have drawn lines indicating the single classical resonance present in H.

Figure 6 shows two eigenstates of the system with β_1 nonzero and the rest of the $\beta_i = 0$. This corresponds to the classical Hamiltonian with only the 2:1 resonance between modes 1 and 2 present. Figure 6a shows a state localized in a region far from the effect of the resonance. Is made up predominantly of a single basis state; the contour plot indicates that the state is centered on a single grid point (n_1, n_2). Figure 6b shows another eigenstate that is strongly affected by the resonance zone. In this case, the state is spread out over a number of the basis states.

In Fig. 7, we show two eigenstates of the system with β_3 as the only nonzero coupling constant. Here, a 2:1 resonance exists between modes 2 and 3. Figure 7a shows a state that is not strongly affected by the resonance, while Fig. 7b gives a state that is situated in the region corresponding to resonant classical dynamics. Again, the nonresonant state is made up almost exclusively of a single basis state, while the resonant state is delocalized over a number of basis states.

For a single resonance term $f_{\mathbf{k}}(\mathbf{I})\cos(\mathbf{k}\cdot\boldsymbol{\theta})$ appearing in the classical Hamiltonian, the time variations of the zeroth-order action vector $\mathbf{I}$ are in the direction of $d\mathbf{I}/dt = -\nabla_{\theta} H(\mathbf{I}, \boldsymbol{\theta})$, which is proportional to the vector $\mathbf{k}$. The quantum state associated with this resonance is delocalized in the same direction: along $\mathbf{k}$ in quantum number space. This is the quantum analogue of the large periodic oscillations of the zeroth-order actions occurring in a Hamiltonian with a single resonance. The classical system is integrable in

this case, and no global energy transport is possible. Likewise, the states of the single resonance quantum Hamiltonian are limited in their extent of delocalization, and none of the signatures of "quantum chaos"[37] are expected to exist for this system.

In Figs. 8a–8d we show four eigenstates of the system with all three

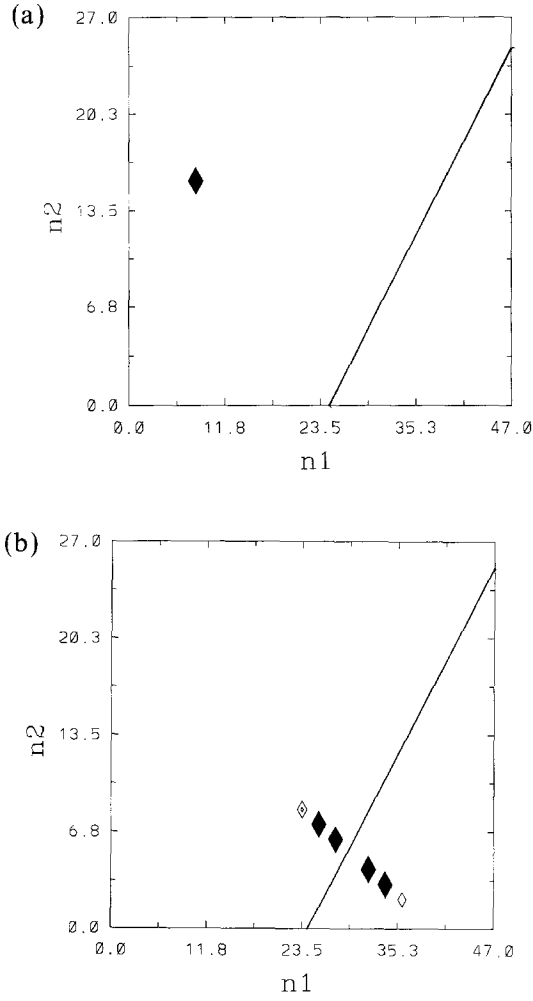

Fig. 6. Contour plots of $\rho(n_1, n_2)$ for two eigenstates of the single-resonance version of Eqs. (25) and (26), with a 2:1 resonance between modes 1 and 2. The center of the classical resonance is indicated by a line on the figure. (a) A state that is far from the classical resonant region, and is localized on a single zeroth-order basis state. (b) A state situated in the classical resonance region. The state is spread over several basis states along the direction **k**. See text for further details.

resonance terms present. We have indicated the centers of the corresponding classical resonances as lines on the plots. The eigenstates all show a greater extent of delocalization than in the integrable single-resonance case. These states are spread over basis states along the direction of **k** for the appropriate resonance, as in the systems having a single resonance term. In

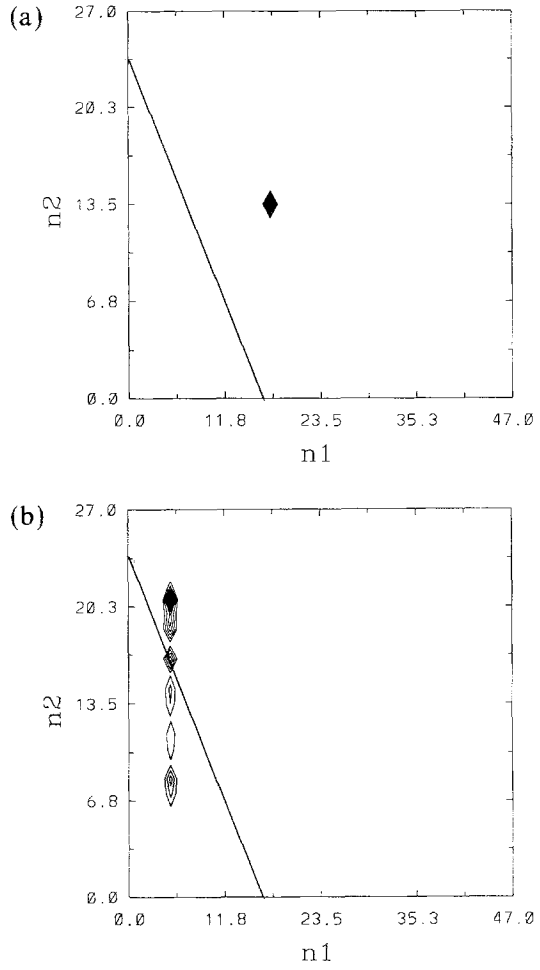

Fig. 7. Contour plots of $\rho(n_1, n_2)$ for two eigenstates of the single-resonance version of Eqs. (25) and (26), with a 2:1 resonance between modes 2 and 3. The center of the classical resonance is indicated by a line on the figure. (a) A state that is far from the classical resonant region, and is localized on a single zeroth-order basis state. (b) A state located in the classical resonance region. The state is spread over several basis states along the direction **k**. See text for further details.

addition, though, states are delocalized *along* the resonance lines. This new phenomenon occurring for the full nonintegrable three-resonance system is reminiscent of the classical Arnold diffusion mechanism, where trajectories wander along resonance channels in phase space. If a time-dependent wave packet were to be localized initially at one point along the resonance zone,

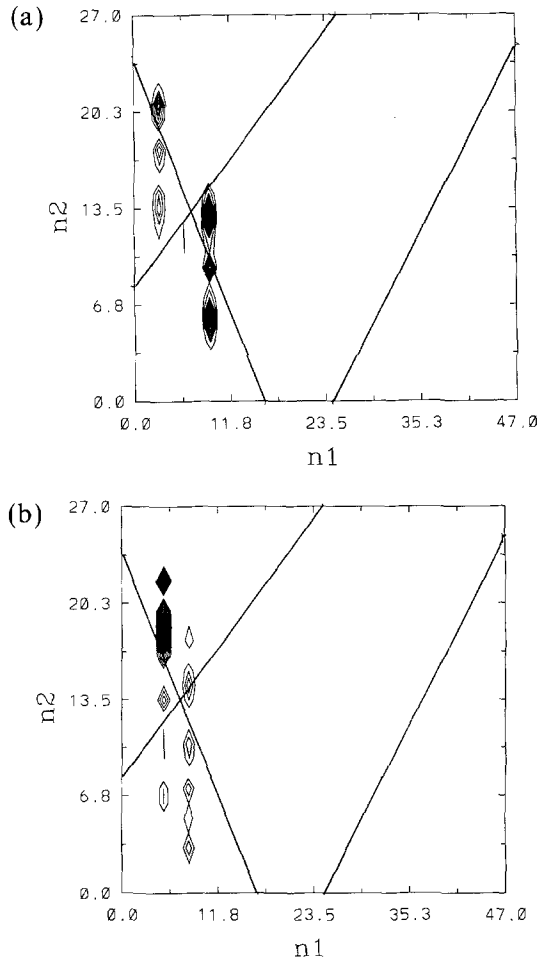

Fig. 8. Contour plots of $\rho(n_1, n_2)$ for four eigenstate of Eqs. (25) and (26), with all three resonance terms present. The centers of the classical resonances have been indicated by lines on the figure. (a)–(c) Three states that are situated in the 2:1 resonances zone between modes 2 and 2, and are delocalized *along* the resonance line, in a manner reminiscent of classical Arnold diffusion. (d) A state showing a similar effect, but in the 2:1 resonance zone between modes 1 and 2. See text for further details.

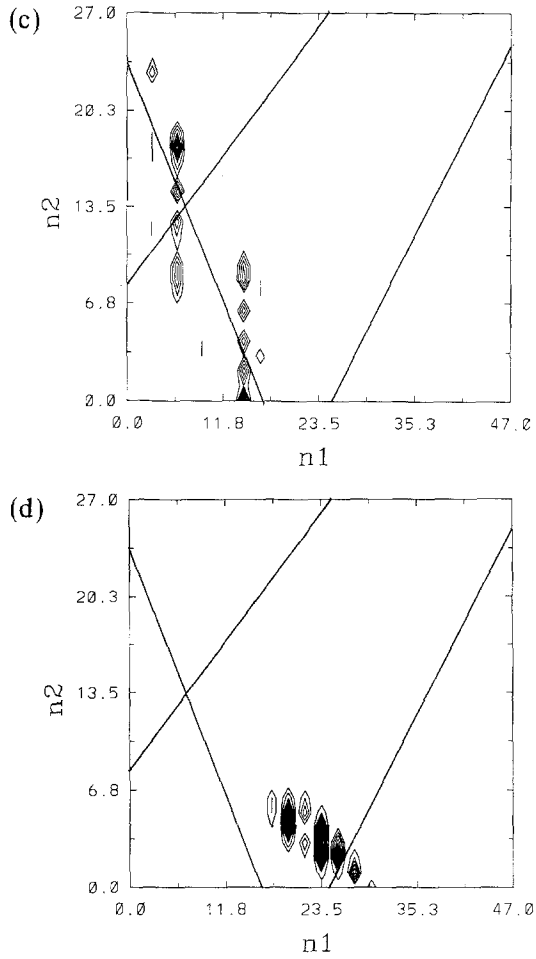

Fig. 8. (*Continued*)

it would flow, as time progressed, along the resonance channel, in much the same way that the classical Arnold web allows energy transport long resonance lines. Figures 8a–8c show three states associated with the 2:1 resonance between modes 2 and 3 that exhibit this delocalization. Figure 8d displays a similar effect, but along the 2:1 resonance between modes 1 and 2.

These preliminary results indicate a delocalization of the quantum states of a three-degree-of-freedom system that appears to be a close analogue of the classical process of transport along resonances in multi-dimensional phase space. We are continuing to investigate the details of

classical–quantum correspondence in this and other systems with $N \geqslant 3$ degrees of freedom[38] and comparing the results with recent formal work.[39]

7. DISCUSSION

In this paper, we have described an approach to the study of classical–quantum correspondence based on the qualitative viewpoint of dynamical systems. We have discussed an extension of quantum surface-of-section methodology to allow nonoscillator problems to be treated, based on the use of generalized coherent states associated with arbitrary Lie groups. We outlined the general approach, and illustrated the method by using the example of $SU(2)$ coherent states to define a quantum surface of section for systems involving rotational degrees of freedom. Two examples involving vibration–rotation interaction in polyatomic molecules were considered; in both cases, strong correlations between classical phase space structure and quantum eigenstate density were observed.

We then presented recent results obtained in our efforts to extend qualitative analysis to classical–quantum correspondence in many-dimensional systems, where the conventional surface-of-section method is not applicable. We considered a model Hamiltonian describing three coupled anharmonic oscillators, and visualized the quantum eigenstates in the quantum analogue of classical action space. The structure of eigenstates in integrable single-resonance versions of the system were interpreted in light of the oscillation of zeroth-order actions in or near nonlinear resonance zones. Additional delocalization of the eigenstates *along* the classical resonances was observed for the fully coupled nonintegrable system, showing a quantum phenomenon reminiscent of classical Arnold diffusion.

Advances in computer technology are providing a steady increase in the size and complexity of physical problems that can be addressed by direct numerical simulation. However, the ability to simulate a problem is not equivalent to gaining physical insight and deep understanding. The data generated by "numerical experiments" must be analyzed and interpreted. The qualitative methods described here for analyzing the results of large-scale quantum calculations of vibration–rotation structure of polyatomic molecules are of potential value in gaining such understanding. Efforts are underway to extend these methods to the analysis of realistic calculations of molecular vibration–rotation eigenstates.

The approach outlined here also has relevance to questions regarding the extent to which appealing classical nonlinear dynamical mechanisms can be employed with confidence in the treatment of inherently quantum mechanical molecular dynamics. Our results suggest that the recent

models and insight provided by nonlinear dynamics[36] are valuable in understanding the properties of the stationary states and dynamics of highly excited molecules, at least at a qualitative level. A qualitative study of *classical* dynamics and phase space structure thus can give useful information about the corresponding *quantum* dynamics and eigenstates of the system.

On a more fundamental level, qualitative understanding of the nature of the quantum mechanics of nonlinear dynamical systems is a key ingredient in continuing work directed at extending the correspondence principle to nonintegrable and chaotic systems.[37,40] The detailed features of classical phase space, and the extent to which they are reflected in the corresponding quantum eigenstates, are of central importance to recent efforts aimed at developing formal quantum and semiclassical theories of classically nonintegrable systems.[37] Such theories attempt to establish connections between classical quantities and related features in the quantum energy spectrum or state space. The results of numerical investigations, such as those described here, provide guidance for these analytic formulations, and suggest which classical phase space structures—periodic orbits, invariant manifolds, or others—should play a central role in the analytical mechanics of classical–quantum correspondence.

ACKNOWLEDGMENTS

We gratefully acknowledge the donors of the Petroleum Research Fund, administered by the American Chemical Society, the NSF Presidential Young Investigator program, and Digital Equipment Corporation for support of this research. We also thank the University of California, Irvine, for an allocation of time on the Convex C240, where many of these calculations were performed.

REFERENCES

1. R. Abraham and J. E. Marsden, *Foundations of Mechanics* (Addison-Wesley, 1985).
2. E. T. Whittaker, *A Treatise on the Analytical Dynamics of Particle and Rigid Bodies* (Cambridge University Press, Cambridge, 1959).
3. H. Poincaré, *Les Méthodes Nouvelles de la Mécanique Celeste* (Dover, 1957).
4. V. I. Arnold, *Mathematical Methods of Classical Mechanics* (Springer, New York, 1978); A. J . Lichtenberg and M. A. Lieberman, *Regular and Stochastic Motion* (Springer, Berlin, 1983); J. Guckenheimer and P. Holmes, *Nonlinear Oscillations, Dynamical Systems, and Bifurcations of Vector Fields* (Springer, New York, 1983); S. N. Rasband, *Chaotic Dynamics of Nonlinear Systems* (Wiley, New York, 1990).

5. V. I. Arnold, *Sov. Math. Dokl.* **5**:581 (1964); B. V. Chirikov, *Phys. Rep.* **52**:265 (1979); J. Tennyson, *Physica* **5D**:123 (1982); P. J. Holmes and J. E. Marsden, *J. Math. Phys.* **23**:669 (1983); K. Kaneko and R. J. Bagley, *Phys. Lett.* **110A**:435 (1985); B. P. Wood, A. J. Lichtenberg, and M. A. Lieberman, *Phys. Rev.* **42A**:5885 (1990).
6. C. C. Martens, M. J. Davis, and G. S. Ezra, *Chem. Phys. Lett.* **142**:519 (1987).
7. C. Cohen-Tannoudji, B. Diu, and F. Laloe, *Quantum Mechanics* (Wiley, New York, 1977).
8. C. C. Martens, *J. Chem. Phys.* **90**:7064 (1989).
9. C. C. Martens, *J. Chem. Phys.* **94**:3594 (1991).
10. C. C. Martens, *J. Chem. Phys.* **96**:1870 (1992).
11. E. J. Heller, *Phys. Rev. Lett.* **53**:1515 (1984); B. Eckhardt, G. Hose, and E. Pollak, *Phys. Rev. A* **39**:3776 (1989).
12. R. M. Stratt, N. C. Handy, and W. H. Miller, *J. Chem. Phys.* **71**:3311 (1979); N. De Leon, M. J. Davis, and E. J. Heller, *J. Chem. Phys.*, **80**:794 (1984).
13. E. P. Wigner, *Phys. Rev.* **40**:749 (1932).
14. K. Husimi, *Proc. Phys. Math. Soc. Japan* **22**:264 (1940).
15. J. R. Klauder and B. Skagerstam, eds., *Coherent States* (World Scientific, Singapore, 1985); W.-M. Zhang, D. H . Feng, aind R. Gilmore, *Rev. Mod. Phys.* **62**:8676 (1990).
16. J. S. Hutchinson and R. E. Wyatt, *Chem. Phys. Lett.* **72**:378 (1980).
17. Y. Weissmann and J. Jortner, *Chem. Phys. Lett.* **78**:224 (1981); Y. Weissman and J. Jortner, *Phys. Lett.* **83A**:55 (1981); Y. Weissman and J. Jortner, *J. Chem. Phys.* **77**:1486 (1982).
19. S.-J. Chang and K.-J. Shi, *Phys. Rev. Lett* . **55**:269 (1985); S.-J. Chang and K.-J. Shi, *Phys. Rev. A* **34**:7 (1986); G. Radons and R. E. Prange, *Phys. Rev. Lett.* **61**:1691 (1988).
20. S. K. Gray, *J. Chem. Phys.* **87**:2051 (1987).
21. W. A. Lin and L. E. Ballentine, *Phys. Lett.* **65**:2927 (1990).
22. R. M. Benito, F. Borondo, J.-H. Kim, B. G. Sumpter, and G. S. Ezra, *Chem. Phys. Lett.* **161**:60 (1989).
23. M. J. Stevens and B. Sundaram, *Phys. Rev. A* **39**:2862 (1989).
24. R. T. Skodje, H. W. Rohrs, and J. VanBuskirk, *Phys. Rev. A* **40**:2894 (1989).
25. R. L. Waterland, J.-M. Yuan, C. C. Martens, and W. P. Reinhardt, *Phys. Rev. Lett.* **61**:2733 (1988).
26. M. Feingold, R. G. Littlejohn, S. B. Solina, J. S. Pehling, and O. Piro, *Phys. Lett. A* **146**:199 (1990).
27. M. J. Davis, C. C. Martens, R. G. Littlejohn, and J. S. Pehling, in *Advances in Molecular Vibrations and Collision Dynamics*, Vol. 1B, J. M. Bowman, ed. (JAI Press, Greenwich, Connecticut, 1991).
28. R. V. Jensen, S. M. Susskind, and M. M. Sanders, *Phys. Rep.* **201**:1 (1991), and references therein.
29. M. E. Kellman and E. D. Lynch, *J. Chem. Phys.* **85**:7216 (1986); L. Xiao and M. E. Kellman, *J. Chem. Phys.* **90**:6086 (1989); M. E. Kellman and L. Xiao, *J. Chem. Phys.* **93**:5821; J. M. Standard and M. E. Kellman, *J. Chem. Phys.* **94**:4714 (1991).
30. M. J. Davis, *J. Phys. Chem.* **92**:3124 (1988).
31. J. Kurchan, P. Leboeuf, and M. Saraceno, *Phys. Rev. A* **40**:6800 (1989).
32. B. G. Wybourne, *Classical Groups for Physicists* (Wiley, New York, 1974).
33. H. Goldstein, *Classical Mechanics* (Addison-Wesley, Reading, Massachusetts, 1980).
34. D. Papousek and M. R. Aliev, *Molecular Vibrational-Rotational Spectra* (Elsevier/North-Holland, New York, 1982).
35. J. Schwinger, in *Quantum Theory of Angular Momentum*, L. C. Biedenharn and H. van Dam, eds. (Academic, New York, 1965); H. V. McIntosh, *Am. J. Phys.* **27**:620

(1959); J. M. Jaunch and E. L. Hill, *Phys. Rev.* **57**:641 (1940); V. A. Dulock and H. V. McIntosh, *Am. J. Phys.* **33**:109 (1965); P. Stehle and M. Y. Han, *Phys. Rev.* **159**:1076 (1967); H. V. McIntosh, in *Group Theory and Its Appli*cations *II*, E. M. Loebl, ed. (Academic Press, New York, 1971).
36. R. S. MacKay and J. D. Meiss, eds. *Hamiltonian Dynamical Systems* (Adam Hilger, Bristol, England, 1987).
37. M. C. Gutzwiller, *Chaos in Classical and Quantum Mechanics* (Springer, New York, 1991), and references therein.
38. Z. Li and C. C. Martens, in preparation.
39. D. Logan and P. G. Wolynes, *J. Chem. Phys.* **93**:4994 (1990).
40. B. L. van der Waerden, ed., *Sources of Quantum Mechanics* (Dover, New York, 1968).